Cancer Letters 440–441 (2019) 106–115

Contents lists available at ScienceDirect

Cancer Letters

journal homepage: www.elsevier.com/locate/canlet

Original Articles

Human UTP14a promotes colorectal cancer progression by forming a positive regulation loop with c-Myc

Jingyi Zhang[a,1], Pengwei Ren[b,1], Da Xu[a,1], Xiaofeng Liu[a], Zhenzhen Liu[a], Chunfeng Zhang[c], Yuan Li[a], Lijun Wang[a], Xiaojuan Du[b,**], Baocai Xing[a,*]

[a] Key Laboratory of Carcinogenesis and Translational Research (Ministry of Education), Hepatopancreatobiliary Surgery Department I, Peking University Cancer Hospital & Institute, No. 52, Fu-Cheng Road, Beijing 100142, China
[b] Department of Cell Biology, School of Basic Medical Sciences, Peking University Health Science Center, Beijing, 100191, China
[c] Department of Medical Genetics, School of Basic Medical Sciences, Peking University Health Science Center, Beijing, 100191, China

ARTICLE INFO

Keywords:
hUTP14a
c-Myc
Protein degradation
Colorectal cancer

ABSTRACT

Nucleolar protein hUTP14a is required for 18S rRNA processing and promotes p53 degradation. Here, we report that hUTP14a stabilizes c-Myc in colorectal cancer (CRC) progression. Firstly, nucleolar hUTP14a is upregulated in human CRC tissues. Mass spectrometry analysis identified c-Myc and its deubiquitinase ubiquitin-specific protease 36 (USP36) in the hUTP14a-specific complex. Importantly, hUTP14a interacts with c-Myc and protects c-Myc from ubiquitination and degradation in a USP36-dependent way. We further demonstrate that hUTP14a forms a complex with USP36/Fbw7γ to inhibit Fbw7γ-mediated c-Myc degradation. Ectopic expression of Flag-hUTP14a enriches c-Myc in the nucleolus, indicating hUTP14a stabilizes c-Myc in the nucleolus. Interestingly, c-Myc activates transcription of hUTP14a. Knockdown of hUTP14a by short hairpin RNA inhibits tumor growth and decreases c-Myc levels in mouse xenografts. Significantly, nucleolar hUTP14a and c-Myc are co-upregulated in human CRC tissues, and this co-upregulation indicates poor prognosis of CRC patients. Thus, disruption of hUTP14a-c-Myc regulation may provide a potential therapeutic strategy for a subset of CRC patients.

1. Introduction

Nucleolar protein hUTP14a is required for 18S rRNA processing [1]. Importantly, hUTP14a binds p53 and promotes p53 degradation, suggesting that hUTP14a might play important roles in human tumorigenesis [1]. Moreover, hUTP14a promotes RB degradation through its E3 ligase activity [2]. Expression of hUTP14a is upregulated in hepatocellular carcinoma and is associated with poor prognosis of the patients [3]. In addition, hUTP14a plays an anti-apoptotic role and protects tumor cells from chemotherapeutic drug-induced apoptosis; thus, hUTP14a might possess a potential as a target in anti-tumor therapy [4].

One of the most important oncoproteins, c-Myc is a transcription factor regulating over 15% of human genes involved in multiple biological processes [5]. c-Myc activates the transcription of downstream genes such as *CCND*, *CDK4*, and *E2F1* to promote cell proliferation [5]. In addition, c-Myc activates rDNA transcription in the nucleolus and plays a pivotal role in regulating ribosome biogenesis and cell growth [6,7]. Gene amplification, chromosomal translocation, and retroviral promoter or enhancer insertion of *MYC* gene are responsible for c-Myc activation in about 20% of human cancers [5]. However, overexpression of c-Myc has been found in about 70% of human tumors [8]. Thus, regulation of c-Myc protein stability plays an essential role in the development of human tumors.

c-Myc is an unstable protein with a half-life of approximately 20 min due to ubiquitin-proteasome system-mediated protein degradation [9–11]. Degradation of c-Myc is mediated by E3 ubiquitin ligases including SKP2, CHIP, TRUSS, and Fbw7γ [12–15]. Inhibition of proteasome-mediated protein degradation leads to c-Myc accumulation in the nucleolus [16,17]. Particularly, Fbw7γ promotes c-Myc

Abbreviations: Colorectal cancer, (CRC); overall survival, (OS); disease-free survival, (DFS); ubiquitin-specific protease, (USP); short hairpin RNA, (shRNA)

* Corresponding author. Key Laboratory of Carcinogenesis and Translational Research (Ministry of Education), Hepatopancreatobiliary Surgery Department I, Peking University Cancer Hospital & Institute, No. 52, Fu-Cheng Road, Beijing 100142, China.

** Corresponding author. Department of Cell Biology, School of Basic Medical Sciences, Peking University Health Science Center, 38 Xue-Yuan Road, Hai-Dian District, Beijing 100191, China.

E-mail addresses: duxiaojuan100@bjmu.edu.cn (X. Du), xingbaocai88@sina.com (B. Xing).

[1] These authors contribute equally to the work.

https://doi.org/10.1016/j.canlet.2018.10.010
Received 7 July 2018; Received in revised form 30 September 2018; Accepted 8 October 2018

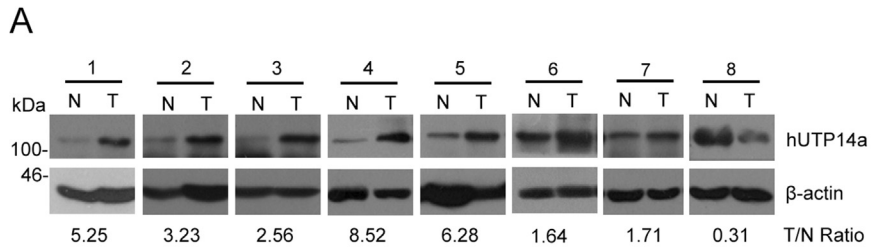

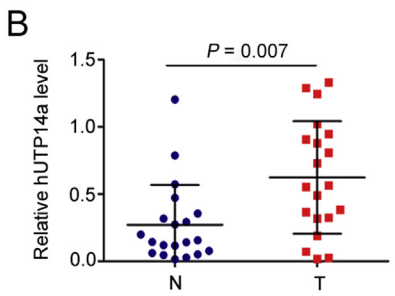

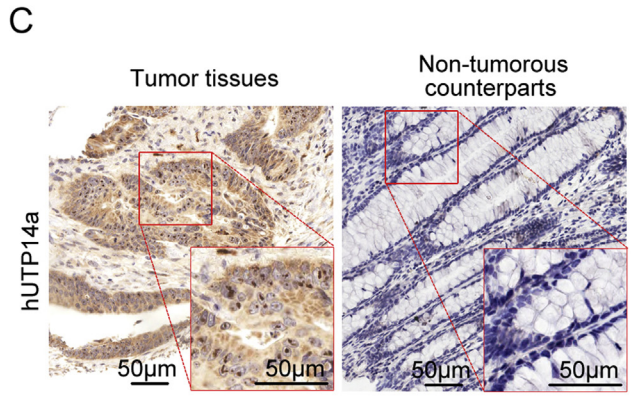

D

hUTP14a expression		Tumor tissues	Non-tumorous counterparts
Negative(%)		10(6.4)	55(35.7)
Positive(%)	Nucleolar	60(39.0)	0(0.0)
	Cytoplasmic	84(54.6)	99(64.3)
Total		154(100.0)	154(100.0)

E

Expression of nucleolar hUTP14a

Tumor tissues	Non-tumorous counterparts			
	Positive(%)	Negative(%)	Total	*P*
Positive(%)	0(0.0)	60(39.0)	60(39.0)	<0.05
Negative(%)	0(0.0)	94(61.0)	94(61.0)	
Total	0(0.0)	154(100.0)	154(100.0)	

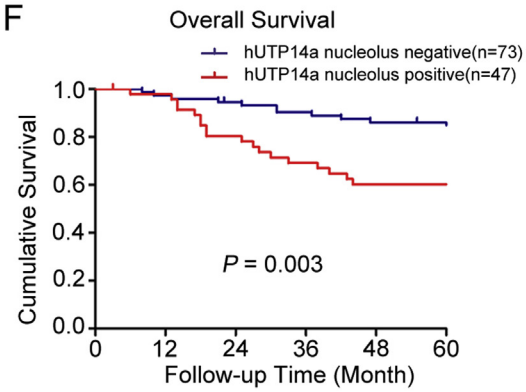

Fig. 1. Nucleolar hUTP14a expression is upregulated in colorectal cancer (CRC) patients. (**A**) Proteins extracted from frozen human colorectal tumor tissues and paired adjacent non-tumorous colorectal tissues were subjected to Western blotting probed with anti-hUTP14a antibody. Beta-actin was used as a loading control (T, tumor tissues; N, non-tumorous counterparts). (**B**) Relative hUTP14a protein levels standardized by β-actin in 20 pairs of CRC tissues and paired adjacent non-tumorous colorectal tissues are shown. (**C**) Representative immunohistochemistry staining of hUTP14a in CRC tissues and adjacent non-tumorous tissues. Scale bars represent 50 μm. (**D**) Summary of hUTP14a expression in 154 pairs of CRC tissues and their non-tumorous counterparts. (**E**) Summary of nucleolar hUTP14a expression in CRC tissues and their non-tumorous counterparts. Pearson's χ^2 test. (**F**) Overall survival of patients with CRC exhibiting different levels of nucleolar hUTP14a expression as determined by Kaplan-Meier analysis. Data are from 120 CRC cases for which survival information was available. $P = 0.003$, log-rank test.

degradation in the nucleolus, and short hairpin RNA (shRNA)-mediated Fbw7γ inhibition leads to nucleolar accumulation of endogenous c-Myc [15]. Recent studies have demonstrated that ubiquitin-mediated degradation of c-Myc was inhibited by USPs including USP28, USP37, and USP36 [18–20]. USP28 and USP37 stabilize c-Myc in the nucleus [18,19], while USP36 interacts with Fbw7γ in the nucleolus and abolishes Fbw7γ- and Fbw7α-mediated c-Myc degradation [20].

Colorectal cancer (CRC) is the third most commonly diagnosed cancer worldwide and the third leading cause of global cancer-related death [21]. Surgical resection could significantly prolong the survival of early-staged CRC patients with a 5-year overall survival (OS) rate of 70%–80% [22]. However, 50% of CRC patients develop recurrence and metastasis after operation, leading to poor prognosis of the patients with a median survival time of about 20 months [23]. Thus, exploration of novel prognostic factors for CRC might improve the outcome of CRC patients. c-Myc is frequently over-expressed in CRC [24], and over-expression of c-Myc is associated with poor prognosis of the patients [25]. Loss of c-Myc attenuates tumor progression and oral administration of c-Myc shRNA improves animal survival in a CRC mouse model. These results suggest that targeting c-Myc will provide a practical therapeutic strategy for CRC [26]. Therefore, exploration of c-Myc regulators may shed light on the cancer therapeutics and improvement of the outcome of CRC patients.

In the present study, we evaluated expression of hUTP14a in CRC and identified c-Myc as an interacting partner of hUTP14a. We thereafter demonstrated that hUTP14a protects c-Myc from degradation by forming a complex with USP36/Fbw7γ in the nucleolus. In turn, c-Myc transactivates hUTP14a transcription. Significantly, co-upregulation of hUTP14a and c-Myc expression predicts poor prognosis of CRC patients.

Table 1
Univariable and multivariable Cox regression analysis of predictive factors of overall survival in I-III stage cases.

Variables	Univariate analysis		Multivariate analysis	
	HR (95% CI)[a]	P[b]	HR (95% CI)[a]	P[b]
Gender				
Male	1			
Female	0.8 (0.4–1.6)	0.544	–	–
Age (y)				
≤60	1			
> 60	0.8 (0.4–1.5)	0.487	–	–
Tumor location				
Colon	1			
Rectum	1.42 (0.7–2.8)	0.321	–	–
Serum CEA level (ng/mL)				
≤5	1		1	
> 5	2.7 (1.3–5.4)	**0.006**	2.4 (1.2–4.8)	**0.017**
CA199 (U/mL)				
≤37	1			
> 37	2.0 (0.9–4.5)	0.081	–	–
Tumor size (cm)				
≤4	1			
> 4	1.5 (0.8–2.8)	0.272	–	–
Tumor differentiation				
Well-moderate	1			
Poor-moderate	1.0 (0.5–2.2)	0.938	–	–
T stage				
T0-3	1			
T4	1.9 (0.87–4.0)	0.110	–	–
N stage				
N0	1			
N1-2	6.2 (2.4–16.1)	< **0.001**	4.7 (1.7–12.9)	**0.002**
Lympho-vascular invasion				
Negative	1			
Positive	3.3 (1.7–6.5)	< **0.001**	–	–
Nucleolar hUTP14a				
Negative	1			
Positive	2.7 (1.4–5.2)	**0.004**	2.8 (1.4–5.7)	**0.003**
c-Myc expression				
Negative	1			
Positive	1.8 (0.8–3.8)	0.131	–	–

[a] Hazard ratios (HRs) and 95% confidence intervals (CIs) were calculated using univariate or multivariate Cox proportional hazards regression in SPSS 17.0.

[b] P values were calculated using univariate or multivariate Cox proportional hazards regression in SPSS 17.0. $P < 0.05$ or $P < 0.01$ were considered to be statistically significant.

2. Materials and methods

2.1. Plasmids and reagents

Expression plasmids encoding pCI-neo-Flag-c-Myc, pCI-neo-Flag-USP36, and pCI-neo-Flag-Fbw7γ were obtained by reverse transcription-polymerase chain reaction (RT-PCR) cloning using total RNA extracted from HeLa cells as a template. Constructed plasmids were verified by DNA sequencing. Lentivirus vector pLKO.1 and the packaging vectors pMD2.G and psPAX2 were purchased from Addgene. Polybrene was purchased from Sigma. MG132 was purchased from Calbiochem. Cycloheximide was purchased from Sigma. Anti-c-Myc (9E10 and C33) and anti-β-actin (1615) antibodies were purchased from Santa Cruz Biotechnology. Anti-HA (H6908), anti-Fbw7γ (F1930), and anti-Flag (3165 and 1804) antibodies were purchased from Sigma. Anti-USP36 (72243) antibody was from Abcam. Anti-hUTP14a antibody was generated in our laboratory [1].

2.2. Patients, tumor tissues, and tissue microarrays

Human CRC tissues and adjacent non-tumorous colorectal tissues used for Western blotting were obtained from 20 CRC patients who underwent tumor resection at Peking University First Hospital from 2003 to 2005. The patients did not receive chemotherapy or irradiation therapy before the operation.

Tissue microarrays consist of 154 formalin-fixed, paraffin-embedded CRC tissues and non-tumorous colorectal tissues obtained from the CRC patients who underwent curative surgical resection without prior neoadjuvant therapy from January 2004 to December 2008 in Beijing Cancer Hospital. The clinical pathologic characteristics of patients including age, gender, tumor location, carcinoembryonic antigen (CEA) level, carbohydrate antigen 19-9 (CA19-9) level, tumor size, tumor differentiation, T stage, N stage, lymphovascular invasion, distant metastasis, and metastatic site are summarized in Supplementary Table S1. The patients included 89 men and 65 women, with a median age of 64 years (range, 22–84 years). The median duration of follow-up time was 69.5 months (range, 2–122 months). Approximately 77.9% (120/154) of patients had stages I–III CRC and 22.1% (34/154) had stage IV CRC with liver-limited metastases (American Joint Committee on Cancer Staging Manual, seventh edition). Adjuvant chemotherapy was given in patients with stage III or more advanced tumor stage. The OS and disease-free survival (DFS) in patients with stages I–III CRC were evaluated. Recurrence occurred in 30.8% (37/120) of patients, and 27.5% (33/120) died of recurrence during the follow-up period.

All human tissues were collected in accordance with the protocols approved by the Ethics Committee of the Peking University Health Science Center, and informed consent was obtained from all patients.

2.3. Immunohistochemistry and evaluation

Immunohistochemistry (IHC) was performed as previously described [27] using anti-hUTP14a and anti-c-Myc antibodies. Results of IHC were determined by two independent pathologists blinded to the clinical outcome. The immunostaining was categorized into four groups: negative (−), 0%–10% positive cells; weakly positive (+), 10%–25% positive cells; moderately positive (++), 25%–50% positive cells; or highly positive (+++), ≥50% positive cells.

2.4. Cell culture, transfection, and luciferase assays

U2OS cell was obtained from the Institute of Basic Medical Sciences, Chinese Academy of Medical Sciences. HeLa and 293T cells were purchased from the American Type Culture Collection. HCT116 $p53^{-/-}$ and HCT116 $p53^{+/+}$ cells were precious gifts from Professor Roland Schuele (Center for Clinical Research, Freiburg University Medical Center, Germany). All of the cells were recently authenticated by Short Tandem Repeat profiling by Shanghai Biowing Applied Biotechnology Company. Microbiological culture was performed to screen all cell lines for mycoplasma contamination. Cell lines were kept frozen and were passaged in the laboratory for fewer than 4 months after resuscitation. All cells were grown in DMEM medium supplemented with 10% fetal bovine serum.

Small interference RNAs (siRNAs) against hUTP14a, c-Myc, and USP36 were used as described previously [1,6,20]. The synthesized siRNA was transfected into cells with Lipofectamine 2000™ (Invitrogen) according to the manufacturer's instructions. Luciferase assay was performed according to the manufacturer's instruction (Promega).

2.5. Immunoprecipitation

Immunoprecipitation was performed as previously described [1,28]. Briefly, cell lysates were prepared in buffer A (25 mM Tris-Cl, pH 7.5, 100 mM KCl, 1 mM dithioerythritol, 2 mM ethylenediaminetetraacetic acid, 0.5 mM phenylmethylsulfonyl fluoride, and 0.1% Nonidet P-40) and used directly for immunoprecipitation. Antibodies were coupled with a 50% suspension of protein A-Sepharose beads (GE Healthcare) in IPP500 (500 mM NaCl, 10 mM Tris-Cl, pH 8.0, and 0.1% Nonidet P-40). Coupled beads were incubated with cell lysates for 2 h at 4 °C. After

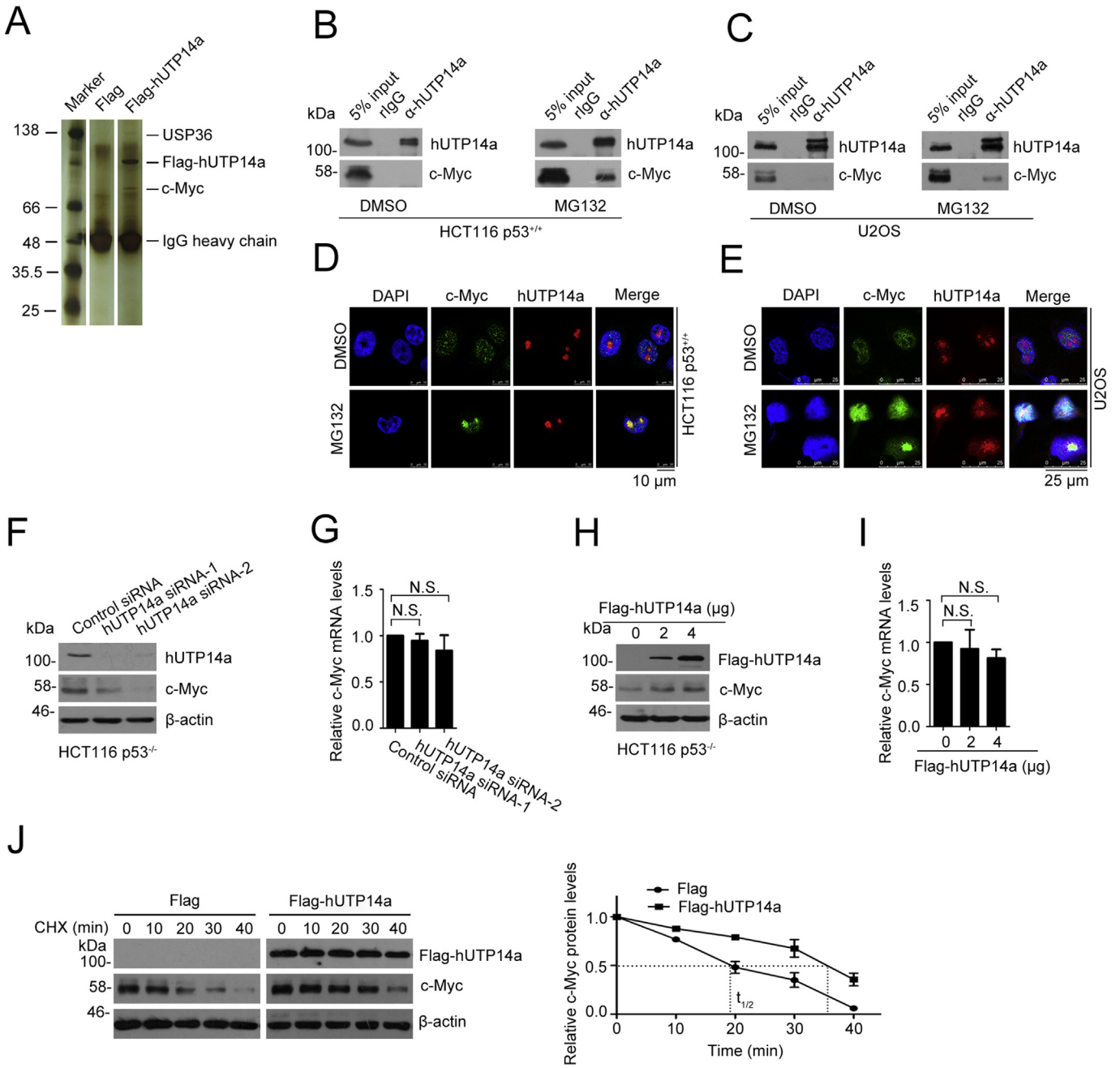

Fig. 2. hUTP14a protected c-Myc through ubiquitin-proteasome pathway. (**A**) Flag-hUTP14a or Flag control vector was transfected into HCT116 $p53^{-/-}$ cells, and immunoprecipitation was performed with an anti-Flag antibody. Proteins from precipitates were separated by SDS-PAGE and detected by silver staining. The hUTP14a-specific bands were subjected to mass spectrometry analysis (**B**), and (**C**) immunoprecipitation was performed with an anti-hUTP14a antibody on HCT116 $p53^{+/+}$ (**B**) and U2OS (**C**) cell lysates. Cells were treated with DMSO or MG132 for 6 h prior to harvest. Proteins from the precipitates were subjected to Western blotting probed with the indicated antibodies. Rabbit IgG (rIgG) was used as an antibody control for immunoprecipitation. (**D**) and (**E**) Cells were treated with DMSO or MG132 for 6 h prior to immunofluorescence staining. Immunofluorescence staining was performed with anti-c-Myc (mouse) and anti-hUTP14a (rabbit) antibodies on HCT116 $p53^{+/+}$ (**D**) and U2OS (**E**) cells. Nuclei were stained with DAPI. Immunofluorescence images were captured using a confocal microscope. Scale bars represent 10 μm (HCT116 $p53^{+/+}$) or 25 μm (U2OS). (**F**) and (**G**) HCT116 $p53^{-/-}$ cells were transfected with hUTP14a siRNAs or control siRNA. Protein and mRNA were extracted and subjected to Western blot (**F**) or RT-qPCR (**G**), respectively. Data are expressed as means ± SEM of three independent experiments. N.S. means no significance, Mann-Whitney *U* test. (**H**) and (**I**) HCT116 $p53^{-/-}$ cells were transfected with indicated amounts of Flag-hUTP14a plasmid. Western blot (**H**) and RT-qPCR (**I**) were performed as described in (**F**) and (**G**). Data were expressed as means ± SEM of three independent experiments. N.S. means no significance, Mann-Whitney *U* test. (**J**) HCT116 $p53^{-/-}$ cells were transfected with indicated plasmids. Cells were harvested at the indicated time points after cycloheximide (CHX) treatment. c-Myc protein levels were evaluated by Western blotting. Relative c-Myc protein levels standardized by β-actin are shown (right).

washing, precipitates were analyzed by Western blot using the indicated antibodies.

2.6. Real-time quantitative PCR

Real-time qPCR was performed using the SYBR-Green qPCR master mix (Roche). *GAPDH* was used as a control for sample normalization. The primers for PCR were as follows: sense primer for *MYC*: 5′-CTC TGA

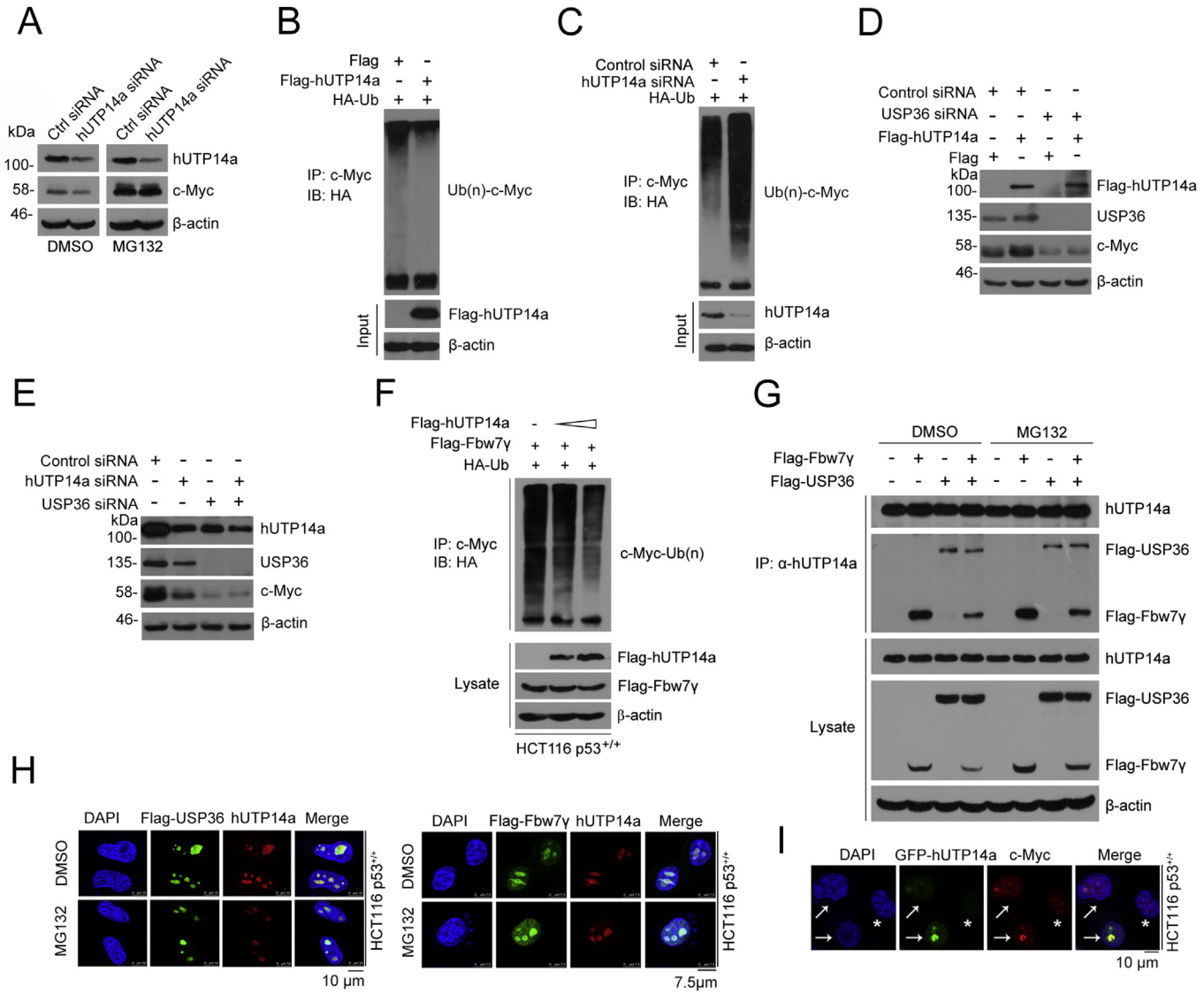

Fig. 3. hUTP14a protects c-Myc from degradation by forming a complex with USP36/Fbw7γ. (**A**) U2OS cells were transfected with siRNAs and treated with MG132 for 6 h at 48 h post-transfection. Proteins from cell lysates were subjected to Western blotting to evaluate indicated proteins. (**B**) U2OS cells were transfected with indicated plasmids. Cells were harvested after treatment with MG132 for 6 h. Immunoprecipitation was performed with anti-c-Myc antibody on the whole cell lysates. Proteins from precipitates were subjected to Western blotting probed with anti-HA antibody. (**C**) hUTP14a or control siRNAs were transfected into U2OS cells and then transfected with the HA-Ub plasmid. Cells were treated with MG132 for 6 h before harvest. Immunoprecipitation was performed with anti-c-Myc antibody, and proteins in the precipitates were immunoblotted with anti-HA antibody. (**D**) U2OS cells were transfected with Flag-hUTP14a or Flag vector 48 h post-transfection of USP36 siRNA or the control siRNA. Proteins from cell lysates were subjected to Western blotting probed with the indicated antibodies. (**E**) U2OS cells were transfected with hUTP14 siRNA or/and USP36 siRNA. Proteins from cell lysates were subjected to Western blotting probed with the indicated antibodies. (**F**) HCT116 $p53^{+/+}$ cells were transfected with HA-ubiquitin, Flag-Fbw7γ, and different doses of Flag-hUTP14a. Cells were treated with 10 μM MG132 for 6 h before harvest. Immunoprecipitation was performed with anti-c-Myc antibody, and the precipitates were subjected to Western blotting probed with anti-HA antibody. (**G**) HCT116 $p53^{+/+}$ cells were transfected with Flag-USP36 or/and Flag-Fbw7γ plasmid. Immunoprecipitation was performed with anti-hUTP14a antibody on whole cell lysates after cells were treated with DMSO or MG132. Immunoprecipitates were subjected to Western blotting for evaluation of hUTP14a, Flag-USP36, and Flag-Fbw7γ. Approximately 5% of the cellular extracts for immunoprecipitation were loaded as the input control. (**H**) HCT116 $p53^{+/+}$ cells were transfected with Flag-USP36 or Flag-Fbw7γ plasmid. Cells were treated with DMSO or MG132 for 6 h. Cells were fixed and double immunofluorescence staining was performed with the indicated antibodies. Nuclei were stained with DAPI. Images were obtained under confocal microscopy. Scale bars represent 10 μm. (**I**) HCT116 $p53^{+/+}$ cells were transfected with GFP-hUTP14a plasmid and fixed 24 h post-transfection. Immunofluorescence staining was performed with anti-c-Myc antibody. c-Myc immuno-signals were recognized with Alexa Fluor 594-labeled goat anti-mouse IgG. GFP-hUTP14a were observed under confocal microscope. Cell nuclei were stained with DAPI. Immunofluorescence images were obtained by confocal microscope. The arrows indicate GFP-hUTP14a transfected cells, and the asterisk represents non-transfected cells. Scale bars represent 10 μm.

AAG GCT CTC CTT GCA-3′, antisense primer for *MYC*: 5′-CCG AGT CGT AGT CGA GGT CAT AG-3′, sense primer for *hUTP14*A: 5′-CAA TGA GAA GCG CAA CAT CC-3′, antisense primer for *hUTP14*A: 5′-TAA TGA TAT GGC CTG GCT TGG-3′, sense primer for *GAPDH*: 5′-ACG GAT TTG GTC GTA TTG GG-3′, and antisense primer for *GAPDH*: 5′-CGC TCC TGG AAG ATG GTG AT-3′.

2.7. Immunofluorescence

Immunofluorescence was performed as previously described [1]. Anti-c-Myc (C33, Santa Cruz Biotechnology) and anti-USP36 (72243, Abcam) were used as primary antibodies. Alexa Fluor 594-conjugated goat anti-rabbit IgG and Alexa Fluor 488-conjugated goat anti-mouse

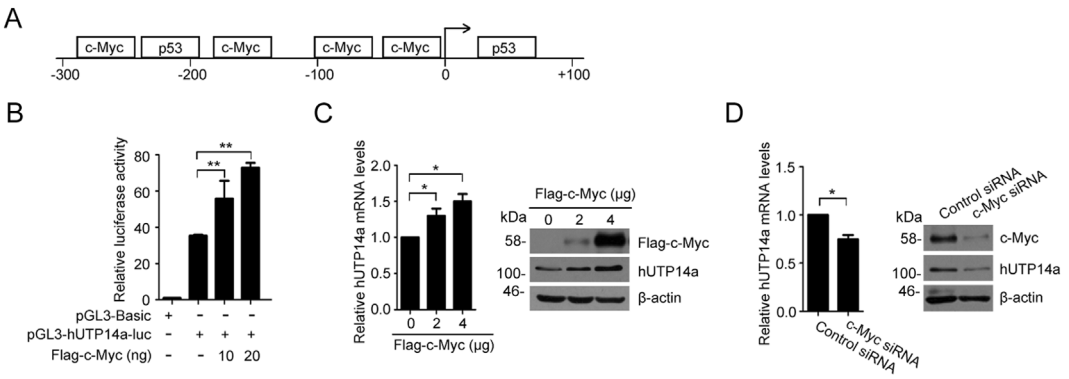

Fig. 4. Transcription of hUTP14a was activated by c-Myc. (**A**) Schematic representation of the putative binding sites of c-Myc and p53 on the hUTP14A promoter. (**B**) hUTP14A promoter reporter plasmid pGL3-hUTP14a-luc was co-transfected with increasing amounts of Flag-c-Myc plasmid into 293T cells in 24-well plates. Luciferase activity was measured 24 h after transfection. Relative luciferase activity is shown. Data are expressed as means ± SEM of three independent experiments in triplicate. Statistical significance was analyzed using one-way analysis of variance (**$P < 0.01$). (**C**) Cells were transfected with the indicated amounts of Flag-c-Myc and harvested 24 h post-transfection. Total RNA was extracted, and RT-qPCR was performed for evaluating the mRNA levels of hUTP14A. Relative hUTP14A mRNA levels are represented by the black histogram (left). Data are expressed as means ± SEM of three independent experiments in triplicate. *$P < 0.05$, Mann-Whitney *U* test. Protein from the cell lysates were subjected to Western blotting (right) to evaluate protein levels of Flag-c-Myc and hUTP14a. (**D**) U2OS cells were transfected with c-Myc siRNA, and control siRNAs. RT-qPCR (left) and Western blot (right) were performed as described in (**C**). Relative hUTP14A mRNA levels are represented by the black histogram. Data are expressed as means ± SEM of three independent experiments in triplicate. *$P < 0.05$, Mann-Whitney *U* test.

IgG (Zhongshan Golden Bridge Biotechnology Co., Ltd) were used as secondary antibodies. Immunofluorescence images were captured using a confocal microscope (Leica TCS-ST2).

2.8. Lentivirus production and shRNA-mediated gene knockdown

The following shRNA sequences were cloned into pLKO.1 vector: control shRNA, 5′-ACU ACC GUU GUU AUA GGU Gtt-3′ and hUTP14a shRNA, 5′-CAG GAA GAA CUA GCG GAU Utt-3′. Lentiviruses for hUTP14a knockdown or scrambled control were generated by transfecting 293T cells with a transducing vector or a control vector, as well as the packaging vectors pMD2.G and psPAX2. Polybrene (8 μg/mL) was added to the medium to improve infection efficiency. The medium was replaced with fresh DMEM supplemented with 10% FBS 12 h after transfection. Virus particles in the medium were collected, filtered, and transduced into target cells 48 h after transfection.

2.9. Mouse xenograft tumor model

Four-to six-week-old female nonobese diabetic/severe combined immunodeficiency (NOD/SCID) mice (Beijing Vital River Laboratory Animal Technology Co., Ltd.) were randomly separated into two groups (n = 5, per group), and HCT116 $p53^{+/+}$ cells expressing pLKO.1-control shRNA or pLKO.1-hUTP14a shRNA (2×10^6) were injected subcutaneously into the right armpit of each mouse. Tumor size was measured with a digital caliper every other day, and the tumor volume was calculated using the formula length × $width^2$ × 0.5 (mm^3). At day 24 post-implantation, the mice were sacrificed. Tumors were collected and weighted. Expression of hUTP14a and c-Myc was evaluated by Western blot. Animal operations were performed according to the National Institutes of Health guidelines. Studies on animals obtained the approval of the Institutional Animal Care and Use Committee of Peking University Health Science Center.

2.10. Statistical analysis

All statistical analyses were carried out using SPSS software 17 version (SPSS Inc.) and GraphPad Prism Software. All data are expressed as means ± SEM. Mann-Whitney *U* test or one-way analysis of variance was used in all cellular experiments to determine statistical significance. The associations between hUTP14a expression and clinical pathological variables were analyzed using the Pearson's χ^2 test. Survival curve was plotted using the Kaplan-Meier method, and the difference between the survival curves was analyzed using the log-rank test. Univariate and multivariate survival analyses were performed using the Cox proportional hazard model. $P < 0.05$ (*), $P < 0.01$ (**), or $P < 0.001$ (***) was considered significant.

3. Results

3.1. Expression of nucleolar hUTP14a is upregulated in CRC patients

To evaluate the expression level of hUTP14a in human CRC tissues, Western blotting was performed on the tumor tissue lysates extracted from CRC tumor and adjacent non-tumorous counterparts. We showed that hUTP14a is upregulated in 16/20 (80%) of CRC tumor tissues compared with their non-tumorous counterparts (Fig. 1A and B). To confirm this finding, the expression of hUTP14a was evaluated by IHC on human CRC tissue's microarray. hUTP14a is detected in the nucleolus (Fig. 1C) and cytoplasm (Supplementary Fig. S1A) in CRC tissues. Nucleolar hUTP14a is significantly upregulated in CRC tumor tissues (60/154, 39.0%) compared with their non-tumorous counterparts (0/154, 0.0%) (Fig. 1D and E, $P < 0.05$). In comparison, no significant difference was found in the cytoplasmic hUTP14a between the CRC tumor tissues (84/154, 54.6%) and their non-tumorous counterparts (99/154, 64.3%) (Fig. 1D and Supplementary Fig. S1B) ($P > 0.05$), indicating that hUTP14a promotes CRC progression mainly through its expression in the nucleolus. To evaluate the significance of nucleolar hUTP14a in the prognosis of CRC patients, Kaplan-Meier survival analysis was conducted based on the nucleolar hUTP14a expression in the primary tumors stages I–III. The OS of the patients with positive nucleolar hUTP14a expression was significantly worse than that of those with negative nucleolar hUTP14a expression (Fig. 1F) ($P < 0.01$). Notably, univariate and multivariate Cox regression analyses showed that besides the serum CEA level and N stage, expression of nucleolar hUTP14a is also considered as an independent prognostic factor for poor survival of CRC patients (Table 1). Furthermore, the nucleolar expression of hUTP14a is positively associated with distant and extra-hepatic metastases ($P < 0.05$) (Supplementary Table S1). However, no significant relationship was found between the nucleolar hUTP14a and gender, age, tumor location, serum CEA level, CA19-9, tumor size, tumor differentiation, T stage, N stage, pathological staging (TNM), or lymphovascular invasion. Thus, hUTP14a may function as a prognostic factor for CRC patients.

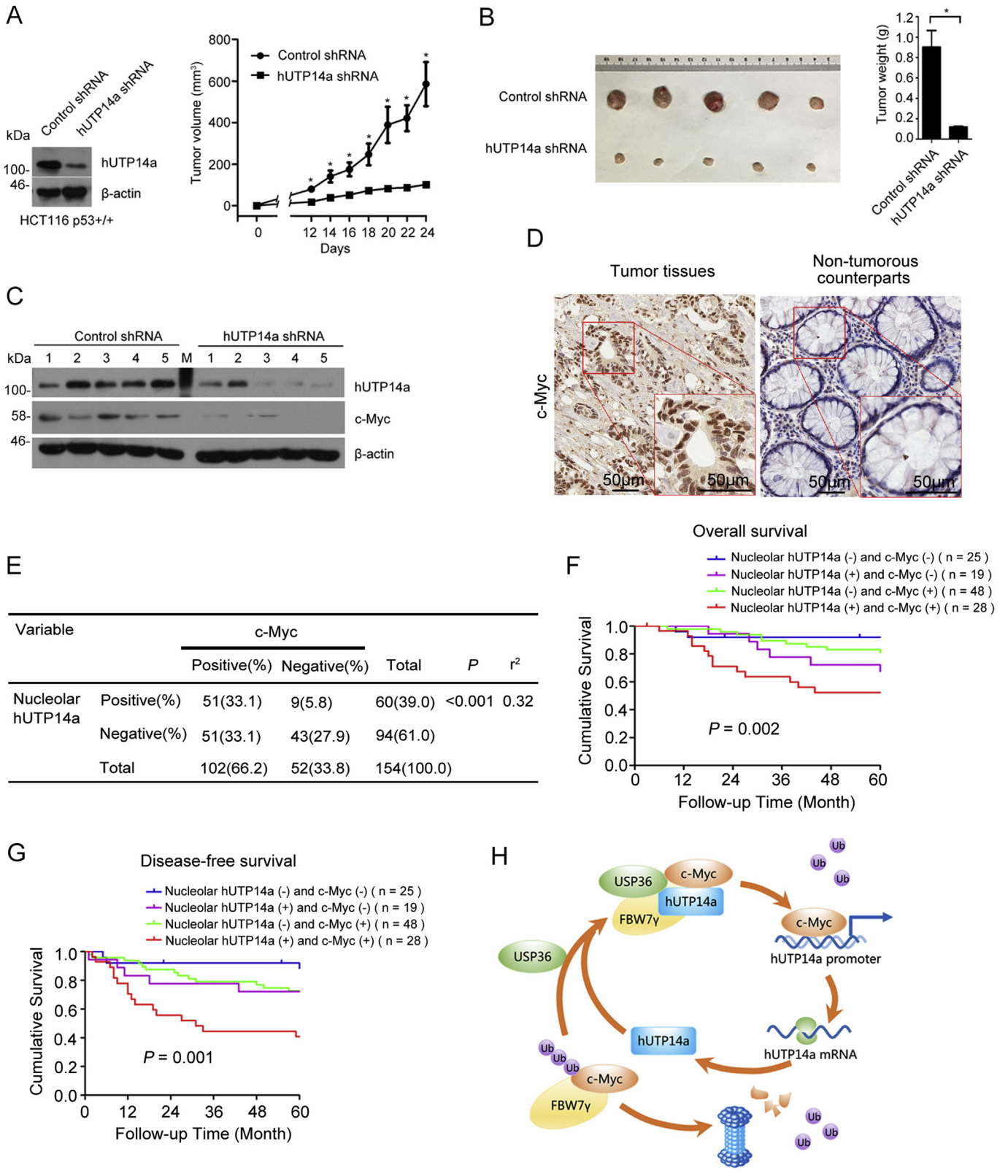

Variable		c-Myc		Total	*P*	r^2
		Positive(%)	Negative(%)			
Nucleolar hUTP14a	Positive(%)	51(33.1)	9(5.8)	60(39.0)	<0.001	0.32
	Negative(%)	51(33.1)	43(27.9)	94(61.0)		
	Total	102(66.2)	52(33.8)	154(100.0)		

(caption on next page)

3.2. hUTP14a interacts with c-Myc

To explore the molecular mechanism by which hUTP14a functions in CRC development, hUTP14a-associated proteins were identified by immunoprecipitation on the cell lysates extracted from CRC cell line HCT116 followed by mass spectrometry analysis. Notably, c-Myc and USP36 were found in the hUTP14a-specific immuno-complex (Fig. 2A). To confirm the interaction between hUTP14a and c-Myc, immunoprecipitation was performed with hUTP14a antibody on HCT116 cell lysates. However, immunoprecipitation showed a faint

Fig. 5. hUTP14a stabilizes c-Myc *in vivo*, and co-upregulation of nucleolar hUTP14a and c-Myc indicates poor prognosis of CRC patients. (**A**) Expression of hUTP14a was evaluated by Western blotting using anti-hUTP14a antibody in HCT116 $p53^{+/+}$ cells stably expressing hUTP14a-shRNA or control shRNA. About 2×10^6 of cells were subcutaneously injected into the right armpit of NOD/SCID mice. Tumor size was measured with a digital caliper every other day, and the tumor volume was calculated as described in the Methods section. Tumor growth curve was plotted using tumor volumes at different time points. (**B**) Mice were sacrificed and tumors were collected 24 days post-implantation (left). Weight of tumors was determined and represented as means ± SEM (right). $^*P < 0.05$, Mann-Whitney *U* test. (**C**) Expression of hUTP14a and c-Myc in the xenograft tumors was evaluated by Western blotting. M means protein marker. (**D**) Representative immunohistochemistry staining of c-Myc in colorectal cancer tissues and adjacent non-tumorous tissues. Scale bars represent 50 μm. (**E**) The correlation between nucleolar hUTP14a and c-Myc in human CRC tissues was analyzed using Spearman's rank correlation test. $P < 0.001$. (**F**) Overall survival curves of CRC patients were plotted against the nucleolar hUTP14a and/or c-Myc expression levels using the Kaplan-Meier method, and the difference between the survival curves was analyzed using the log-rank test. Data were summarized from 120 CRC cases with which survival information was available. (**G**) Disease-free survival curves of CRC patients against the nucleolar hUTP14a and/or c-Myc expression levels was plotted by Kaplan-Meier analysis. Data were summarized from 120 CRC cases with which survival information was available. (**H**) Working model to illustrate the positive regulatory loop between hUTP14a and c-Myc.

interaction between hUTP14a and c-Myc under normal conditions. Since hUTP14a is a nucleolar protein and c-Myc has been found to be accumulated in the nucleolus when proteasomal activity is inhibited [17,29], we thus treated cells with proteasome inhibitor MG132 and performed immunoprecipitation experiments. hUTP14a binds c-Myc in HCT116 and U2OS cells under MG132 treatment (Fig. 2B and C), suggesting that hUTP14a might regulate proteasomal degradation of c-Myc. In addition, c-Myc is co-localized with hUTP14a in the nucleolus upon MG132 treatment in HCT116 $p53^{+/+}$, U2OS, and HeLa cells (Fig. 2D and E and Supplementary Fig. S2), confirming that hUTP14a interacts c-Myc in the nucleolus.

3.3. hUTP14a stabilizes c-Myc through the ubiquitin-proteasome pathway

We thereafter wanted to know if hUTP14a regulates c-Myc protein level. Since hUTP14a promotes p53 degradation [1], we evaluated c-Myc levels when hUTP14a was silenced in the HCT116 $p53^{-/-}$ and U2OS cells. Knockdown of hUTP14a results in decreased levels of c-Myc in the HCT116 $p53^{-/-}$ cells (Fig. 2F) and U2OS cells (Supplementary Fig. S3A), suggesting that hUTP14a regulates c-Myc level regardless of p53 expression. Furthermore, knockdown of hUTP14a did not significantly change the *MYC* mRNA levels (Fig. 2G). Accordingly, ectopic expression of Flag-hUTP14a caused a dose-dependent increase of c-Myc levels in the HCT116 $p53^{-/-}$ (Fig. 2H) and U2OS cells (Supplementary Fig. S3B) without changing the mRNA levels of *MYC* (Fig. 2I). These results indicated that hUTP14a increases c-Myc levels by protein–protein interaction rather than transcriptional regulation.

Thus, we wanted to determine if hUTP14a affects protein stability of c-Myc. The half-life of c-Myc was prolonged to more than 30 min when Flag-hUTP14a was ectopically expressed, whereas it was approximately 20 min in the Flag transfected cells (Fig. 2J) as described previously [11,12], indicating that hUTP14a stabilizes c-Myc protein.

To determine if the hUTP14a-mediated c-Myc stabilization is related to the ubiquitin-proteasome pathway, cells were treated with MG132. Knockdown of hUTP14a-induced c-Myc reduction was inhibited by MG132, indicating that hUTP14a stabilizes c-Myc through proteasome-mediated pathway (Fig. 3A). Further, *in vivo* ubiquitination experiments showed that ectopic Flag-hUTP14a inhibits c-Myc polyubiquitination in cells (Fig. 3B). In contrast, knockdown of hUTP14a results in increased c-Myc ubiquitination (Fig. 3C), demonstrating that hUTP14a stabilizes c-Myc by inhibiting ubiquitination of c-Myc.

3.4. hUTP14a forms a complex with USP36/Fbw7γ to inhibit Fbw7γ-mediated c-Myc degradation

As USP36 stabilizes c-Myc in the nucleolus [20] and is identified in the hUTP14a-specific protein complex (Fig. 2A), we asked if the hUTP14a-induced c-Myc stabilization is mediated by USP36. The depletion of USP36 dramatically decreases c-Myc levels as previously described [20] (Fig. 3D). Importantly, Flag-hUTP14a failed to upregulate c-Myc in the absence of USP36, demonstrating that hUTP14a-mediated c-Myc stabilization is dependent on USP36. Accordingly, knockdown of hUTP14a causes a significant decrease in c-Myc levels only in the presence of USP36 (Fig. 3E), confirming that USP36 is required for the hUTP14a-mediated c-Myc stabilization. As USP36 protects c-Myc from Fbw7γ-mediated degradation in the nucleolus [20], we evaluated if hUTP14a affects Fbw7γ-mediated c-Myc ubiquitination. Results showed that Flag-hUTP14a inhibits Fbw7γ-mediated c-Myc ubiquitination in a dose-dependent manner (Fig. 3F), demonstrating that hUTP14a stabilizes c-Myc by inhibiting Fbw7γ-mediated c-Myc degradation.

Thereafter, we determined if hUTP14a binds with USP36 and Fbw7γ. We transfected cells with Flag-USP36 or/and Flag-Fbw7γ and performed immunoprecipitation with anti-hUTP14a antibody. Flag-USP36 and Flag-Fbw7γ co-existed in the hUTP14a-specific immunoprecipitates regardless of MG132 treatment, demonstrating that hUTP14a forms a complex with USP36 and Fbw7γ (Fig. 3G). Immunofluorescence staining showed that hUTP14a co-localizes with Flag-USP36 and Flag-Fbw7γ in the nucleolus whether cells were treated with MG132 or not (Fig. 3H), confirming that hUTP14a interacts with USP36 and Fbw7γ in the nucleolus. Importantly, c-Myc was localized in the nucleolus in GFP-hUTP14a expressed cells, whereas c-Myc remained in the nucleoplasm in untransfected cells (Fig. 3I and Supplementary Fig. S4), demonstrating that hUTP14a accumulates c-Myc in the nucleolus. Collectively, we demonstrated that hUTP14a forms a hUTP14a/USP36/Fbw7γ complex to inhibit Fbw7γ-mediated c-Myc degradation in the nucleolus.

3.5. c-Myc activates transcription of hUTP14A

To unravel the mechanism by which hUTP14a is upregulated in CRC, we set out to explore the transcriptional regulation of hUTP14a. The potential upstream regulatory factor(s) of *hUTP14*A promoter was analyzed using a MatInspector Professional program. Both p53 and c-Myc were found to be putative transcription factors in the minimal promoter region of *hUTP14*A gene [30] (Fig. 4A). However, the luciferase activity of the hUTP14a-promoter-luciferase reporter pGL3-hUTP14a-luc was activated by Flag-c-Myc in a dose-dependent manner (Fig. 4B) but not by Flag-p53 [30] (Supplementary Fig. S5A), suggesting that transcription of *hUTP14*A was upregulated by c-Myc. In addition, *hUTP14*A mRNA levels were elevated by Flag-c-Myc (Fig. 4C) but not by Flag-p53 (Supplementary Fig. S5B). Meanwhile, hUTP14a protein levels were elevated by ectopic Flag-c-Myc. Accordingly, knockdown of c-Myc by siRNA caused a dramatic decrease in *hUTP14*A mRNA and hUTP14a protein levels (Fig. 4D). These results demonstrated that c-Myc activates transcription of *hUTP14*A. Thus, hUTP14a forms a positive regulation loop with c-Myc.

3.6. Knockdown of hUTP14a inhibits tumor growth and decreases c-Myc levels in mouse xenografts

To explore the role of hUTP14a in CRC progression, we established a stable cell line with hUTP14a-depleted by shRNA in the HCT116 $p53^{+/+}$ cells (Fig. 5A). HCT116-hUTP14a shRNA cells or HCT116-control shRNA cells were subcutaneously injected into the NOD/SCID mice, respectively. Tumor sizes were monitored every other day. As

shown in Fig. 5A and B, the volume and weight of xenograft tumors derived from HCT116-hUTP14a shRNA cells were significantly smaller than that derived from HCT116-control shRNA cells ($P < 0.05$), demonstrating that knockdown of hUTP14a inhibits CRC growth *in vivo*. We have evaluated the expression levels of hUTP14a, c-Myc, USP36, and Fbw7γ in the mouse xenografts (Fig. 5C and Supplementary Fig. S6). Significantly, depletion of hUTP14a decreased the levels of c-Myc in xenograft tumors, demonstrating that hUTP14a stabilizes c-Myc *in vivo*.

3.7. Nucleolar hUTP14a positively correlates with c-Myc expression in human CRC tissues and co-upregulation of hUTP14a and c-Myc indicates poor prognosis of patients

Thereafter, we evaluated if expression of nucleolar hUTP14a correlates with c-Myc in human CRC tissues. c-Myc was upregulated in CRC tumor tissues (102/154, 66.2%) (Fig. 5D and E) as described previously [24]. Nucleolar hUTP14a was positively correlated with expression of c-Myc ($P < 0.001$) (Fig. 5E), indicating that nucleolar hUTP14a and c-Myc are co-upregulated in a subset of human CRC tumor tissues *in vivo*. Notably, the 5-year OS rate of patients with co-upregulation of nucleolar hUTP14a and c-Myc expression was significantly worse than that of patients with single c-Myc positive expression (52.4% vs 83.1%, $P < 0.01$) and that of the patients expressing neither c-Myc nor nucleolar hUTP14a (52.4% vs 92.0%, $P < 0.01$) (Fig. 5F). The 5-year DFS of patients with co-upregulation of nucleolar hUTP14a and c-Myc expression was worse than that of patients with single nucleolar hUTP14a expression (72.2% vs 92.0%, $P < 0.05$) and single c-Myc positive expression (72.6% vs 92.0%, $P < 0.01$) and that of patients with neither c-Myc nor nucleolar hUTP14a expression (39.4% vs 92.0%, $P < 0.01$) (Fig. 5G). These findings strongly demonstrated that co-upregulation of nucleolar hUTP14a and c-Myc plays a critical role in CRC progression and possesses prognostic potential for the outcome of CRC patients.

4. Discussion

c-Myc plays an essential role in the initiation of CRC since down-regulation of c-Myc inhibits intestinal polyposis, which is the very primary pathological change in the development of CRC [31,32]. In addition, c-Myc promotes progression of CRC [24,33]. Thus, c-Myc-regulators may contribute to tumor initiation and progression [10]. In the present study, we have identified hUTP14a as an important regulator of c-Myc in the progression of CRC.

Here, we initially found that nucleolar hUTP14a is significantly upregulated in human CRC tissues, suggesting that hUTP14a may play a role in the CRC progression through its function in the nucleolus. Interestingly, USP36 and c-Myc are found in the hUTP14a-specific immunoprecipitates in CRC cells. We found that hUTP14a binds c-Myc and stabilizes c-Myc through proteasome-mediated pathway. Interestingly, hUTP14a protects c-Myc from Fbw7γ-mediated degradation in a USP36-dependent manner. We further demonstrate that hUTP14a forms a complex with USP36/Fbw7γ in the nucleolus. Importantly, hUTP14a binds and co-localizes with Flag-USP36 and Flag-Fbw7γ in the nucleolus with or without MG132 treatment, demonstrating that hUTP14a forms a stable complex with USP36 and Fbw7γ. In comparison, hUTP14a binds c-Myc in the nucleolus only when proteasomal activity is blocked, demonstrating that hUTP14a protects c-Myc from degradation in the nucleolus and therefore elevates the cellular level of c-Myc. This is verified by the results showing that c-Myc is accumulated in the nucleolus in the GFP-hUTP14a expressed cells. Collectively, we demonstrate that hUTP14a forms a hUTP14a/USP36/Fbw7γ complex to inhibit c-Myc degradation in the nucleolus (Fig. 5H).

c-Myc promotes cell proliferation by upregulating a large number of downstream genes [5,34,35] such as *CCND1*, *BOP1*, and *PES1* [36–38]. Recently, integrin α1β1, which was shown to be upregulated in 65% of CRC patients and promote colon cancer cell invasion, was found to be regulated by c-Myc in CRC [39]. Thus, identification of downstream genes of c-Myc would provide insights toward understanding the function of c-Myc and provide more targets for clinical therapy of cancers. In the present study, we identified hUTP14a as a downstream gene of c-Myc. Since hUTP14a is required for 18S rRNA processing and promotes p53 and RB degradation [1,2], c-Myc might partially promote CRC progression by activating hUTP14a expression.

Despite the fact that surgical techniques have achieved significant advances over the years, the recurrence and metastasis rate of CRC remain high after curative therapy. Extrahepatic metastasis of CRC is a negative prognostic factor for CRC patients, causing less than 20% of the 5-year OS even after curative treatment [40,41]. In the present study, expression of nucleolar hUTP14a is significantly associated with extrahepatic metastases; thus, interference of hUTP14a expression in the patients with nucleolar hUTP14a expression might improve the outcome of the patients. Several genes have been reported to be related with extrahepatic metastases in CRC patients such as *BRAF* and *KRAS*. *KRAS* gene mutations have been found in 50% of CRC patients, and activation of the downstream genes by mutated *KRAS* expression diminishes the response of the patients to the anti-EGFR drug such as cetuximab [42]. In addition, expression of c-Myc is associated with the presence of *KRAS* and *BRAF* mutations in CRC [43]. Besides, *MYC* might be a downstream gene of KRAS or BRAF [44]. Thus, a regulation loop between c-Myc and KRAS or BRAF may play an important role in CRC progression. Here, we demonstrate that hUTP14a forms a positive regulation feedback loop with c-Myc. Hence, future studies should determine whether hUTP14a is associated with *KRAS* and *BRAF* mutations in CRC.

In the present study, we demonstrate that nucleolar hUTP14a acts as a novel independent prognostic factor for reduced OS of CRC patients. Additionally, nucleolar hUTP14a expression is not correlated with serum CEA level and N stage, which are used as prognostic factors for CRC [45,46]. Thus, evaluation of nucleolar hUTP14a in combination of CEA levels and N stage might help improve the prediction of the prognosis of CRC patients.

Given the demonstrated importance of c-Myc in promoting CRC progression, much effort has been made to target c-Myc for CRC therapy. Notably, several therapeutic targets of CRC identified in a genome-scale analysis of 276 CRC samples reported by the Cancer Genome Atlas all eventually converged on c-Myc [25]. Accordingly, various strategies have been employed to target c-Myc directly or indirectly. Direct inhibitors and indirect interference with c-Myc expression or stability have shown a high therapeutic efficacy for many tumors [47,48]. In the present study, we found that hUTP14a forms a positive regulation loop with c-Myc, raising the possibility that inhibition of hUTP14a expression might provide a clinically tractable path toward the treatment of CRC. Furthermore, co-upregulation of both hUTP14a and c-Myc proteins indicated poor outcome, suggesting that these two proteins may act synergistically in CRC progression. Importantly, depletion of hUTP14a inhibits tumor growth and decreases c-Myc expression levels in mouse xenograft. Thus, inhibition of hUTP14a expression may provide a potential clinical therapeutic strategy for a certain subset of CRC patients expressing nucleolar hUTP14a and c-Myc.

Conflicts of interest

The authors declare no conflict of interest.

Acknowledgments

We're grateful for the grants from the National Natural Science Foundation of China (grant nos. 81371868, 81672735, and 81621063), the 973 Program (grant no. 2013CB837201), and the Innovation Team

of Ministry of Education (IRT13001). We thank Dr. Qihua He for assistance with confocal microscopy. We are grateful for Dr. Bin Dong and Dr. Min Lu for their assistance in immunohistochemistry analysis.

Appendix A. Supplementary data

Supplementary data to this article can be found online at https://doi.org/10.1016/j.canlet.2018.10.010.

References

[1] L. Hu, J. Wang, Y. Liu, Y. Zhang, L. Zhang, R. Kong, Z. Zheng, X. Du, Y. Ke, A small ribosomal subunit (SSU) processome component, the human U3 protein 14A (hUTP14A) binds p53 and promotes p53 degradation, J. Biol. Chem. 286 (2011) 3119–3128.
[2] H. Liu, J. Wang, Y. Liu, L. Hu, C. Zhang, B. Xing, X. Du, Human U3 protein14a is a novel type ubiquitin ligase that binds RB and promotes RB degradation depending on a leucine-rich region, Biochim. Biophys. Acta Mol. Cell Res. 1865 (2018) 1611–1620.
[3] J.Y. Zhang, D. Xu, Z.Z. Liu, Y. Li, L.J. Wang, B.C. Xing, Human U three protein 14a expression is increased in hepatocellular carcinoma and associated with poor prognosis, Chinese Med J 130 (2017) 470–476.
[4] T. Ma, C. Lu, Y. Guo, C. Zhang, X. Du, Human U3 protein 14a plays an anti-apoptotic role in cancer cells, Biol. Chem. 398 (2017) 1247–1257.
[5] N. Meyer, L.Z. Penn, Reflecting on 25 years with MYC, Nat. Rev. Canc. 8 (2008) 976–990.
[6] A. Arabi, S. Wu, K. Ridderstrale, H. Bierhoff, C. Shiue, K. Fatyol, S. Fahlen, P. Hydbring, O. Soderberg, I. Grummt, L.G. Larsson, A.P. Wright, c-Myc associates with ribosomal DNA and activates RNA polymerase I transcription, Nat. Cell Biol. 7 (2005) 303–310.
[7] C. Grandori, N. Gomez-Roman, Z.A. Felton-Edkins, C. Ngouenet, D.A. Galloway, R.N. Eisenman, R.J. White, c-Myc binds to human ribosomal DNA and stimulates transcription of rRNA genes by RNA polymerase I, Nat. Cell Biol. 7 (2005) 311–318.
[8] G. Ciriello, M.L. Miller, B.A. Aksoy, Y. Senbabaoglu, N. Schultz, C. Sander, Emerging landscape of oncogenic signatures across human cancers, Nat. Genet. 45 (2013) 1127–1133.
[9] S.E. Salghetti, S.Y. Kim, W.P. Tansey, Destruction of Myc by ubiquitin-mediated proteolysis: cancer-associated and transforming mutations stabilize Myc, EMBO J. 18 (1999) 717–726.
[10] A.S. Farrell, R.C. Sears, MYC degradation, Cold Spring Harb Perspect Med 4 (2014).
[11] S.R. Hann, R.N. Eisenman, Proteins encoded by the human c-myc oncogene: differential expression in neoplastic cells, Mol. Cell Biol. 4 (1984) 2486–2497.
[12] S.Y. Kim, A. Herbst, K.A. Tworkowski, S.E. Salghetti, W.P. Tansey, Skp2 regulates Myc protein stability and activity, Mol. Cell. 11 (2003) 1177–1188.
[13] I. Paul, S.F. Ahmed, A. Bhowmik, S. Deb, M.K. Ghosh, The ubiquitin ligase CHIP regulates c-Myc stability and transcriptional activity, Oncogene 32 (2013) 1284–1295.
[14] S.H. Choi, J.B. Wright, S.A. Gerber, M.D. Cole, Myc protein is stabilized by suppression of a novel E3 ligase complex in cancer cells, Genes Dev. 24 (2010) 1236–1241.
[15] M. Welcker, A. Orian, J.E. Grim, R.N. Eisenman, B.E. Clurman, A nucleolar isoform of the Fbw7 ubiquitin ligase regulates c-Myc and cell size, Curr. Biol. 14 (2004) 1852–1857.
[16] A. Arabi, Accumulation of c-Myc and proteasomes at the nucleoli of cells containing elevated c-Myc protein levels, J. Cell Sci. 116 (2003) 1707–1717.
[17] Z. Li, S.R. Hann, Nucleophosmin is essential for c-Myc nucleolar localization and c-Myc-mediated rDNA transcription, Oncogene 32 (2013) 1988–1994.
[18] J. Pan, Q. Deng, C. Jiang, X. Wang, T. Niu, H. Li, T. Chen, J. Jin, W. Pan, X. Cai, X. Yang, M. Lu, J. Xiao, P. Wang, USP37 directly deubiquitinates and stabilizes c-Myc in lung cancer, Oncogene 34 (2015) 3957–3967.
[19] N. Popov, M. Wanzel, M. Madiredjo, D. Zhang, R. Beijersbergen, R. Bernards, R. Moll, S.J. Elledge, M. Eilers, The ubiquitin-specific protease USP28 is required for MYC stability, Nat. Cell Biol. 9 (2007) 765–774.
[20] X.X. Sun, X. He, L. Yin, M. Komada, R.C. Sears, M.S. Dai, The nucleolar ubiquitin-specific protease USP36 deubiquitinates and stabilizes c-Myc, Proc. Natl. Acad. Sci. U. S. A. 112 (2015) 3734–3739.
[21] L.A. Torre, F. Bray, R.L. Siegel, J. Ferlay, J. Lortet-Tieulent, A. Jemal, Global cancer statistics, 2012, CA A Cancer J. Clin 65 (2015) 87–108.
[22] T. Andre, C. Boni, M. Navarro, J. Tabernero, T. Hickish, C. Topham, A. Bonetti, P. Clingan, J. Bridgewater, F. Rivera, A. de Gramont, Improved overall survival with oxaliplatin, fluorouracil, and leucovorin as adjuvant treatment in stage II or III colon cancer in the MOSAIC trial, J. Clin. Oncol. 27 (2009) 3109–3116.
[23] S. Kraus, I. Nabiochtchikov, S. Shapira, N. Arber, Recent advances in personalized colorectal cancer research, Cancer Lett. 347 (2014) 15–21.
[24] C.V. Dang, MYC on the path to cancer, Cell 149 (2012) 22–35.
[25] N. Cancer, Genome Atlas, Comprehensive molecular characterization of human colon and rectal cancer, Nature 487 (2012) 330–337.
[26] N.K. Tangudu, V.K. Verma, T.D. Clemons, S.S. Beevi, T. Hay, G. Mahidhara, M. Raja, R.A. Nair, L.E. Alexander, A.B. Patel, J. Jose, N.M. Smith, B. Zdyrko, A. Bourdoncle, I. Luzinov, K.S. Iyer, A.R. Clarke, L. Dinesh Kumar, RNA interference using c-Myc-conjugated nanoparticles suppresses breast and colorectal cancer models, Mol. Canc. Therapeut. 14 (2015) 1259–1269.
[27] K.M. Jin, M. Lu, F.F. Liu, J. Gu, X.J. Du, B.C. Xing, N-WASP is highly expressed in hepatocellular carcinoma and associated with poor prognosis, Surgery 153 (2013) 518–525.
[28] X. Liu, S. Cai, C. Zhang, Z. Liu, J. Luo, B. Xing, X. Du, Deacetylation of NAT10 by Sirt1 promotes the transition from rRNA biogenesis to autophagy upon energy stress, Nucleic Acids Res. 46 (2018) 9601–9616.
[29] A. Arabi, C. Rustum, E. Hallberg, A.P. Wright, Accumulation of c-Myc and proteasomes at the nucleoli of cells containing elevated c-Myc protein levels, J. Cell Sci. 116 (2003) 1707–1717.
[30] J. Zhang, Y. Guo, X. Du, B. Xing, Does not hUTP14a promoter form a regulation feedback loop with P53? Chin. J. Canc. Res. = Chung-kuo yen cheng yen chiu 26 (2014) 159–165.
[31] K. Yekkala, T.A. Baudino, Inhibition of intestinal polyposis with reduced angiogenesis in ApcMin/+ mice due to decreases in c-Myc expression, Mol. Canc. Res. 5 (2007) 1296–1303.
[32] O.J. Sansom, V.S. Meniel, V. Muncan, T.J. Phesse, J.A. Wilkins, K.R. Reed, J.K. Vass, D. Athineos, H. Clevers, A.R. Clarke, Myc deletion rescues Apc deficiency in the small intestine, Nature 446 (2007) 676–679.
[33] X. Zhang, Y.L. Ge, R.H. Tian, The knockdown of c-myc expression by RNAi inhibits cell proliferation in human colon cancer HT-29 cells in vitro and in vivo, Cell. Mol. Biol. Lett. 14 (2009) 305–318.
[34] A. Borriello, D. Bencivenga, M. Criscuolo, I. Caldarelli, V. Cucciolla, A. Tramontano, A. Borgia, A. Spina, A. Oliva, S. Naviglio, F. Della Ragione, Targeting p27Kip1 protein: its relevance in the therapy of human cancer, Expert Opin. Ther. Targets 15 (2011) 677–693.
[35] G. Wu, M. Yuan, S. Shen, X. Ma, J. Fang, L. Zhu, L. Sun, Z. Liu, X. He, Huang, T. Li, C. Li, J. Wu, X. Hu, Z. Li, L. Song, K. Qu, H. Zhang, P. Gao, Menin enhances c-Myc-mediated transcription to promote cancer progression, Nat. Commun. 8 (2017) 15278.
[36] P.C. Fernandez, S.R. Frank, L. Wang, M. Schroeder, S. Liu, J. Greene, A. Cocito, B. Amati, Genomic targets of the human c-Myc protein, Genes Dev. 17 (2003) 1115–1129.
[37] I. Schlosser, M. Holzel, M. Murnseer, H. Burtscher, U.H. Weidle, D. Eick, A role for c-Myc in the regulation of ribosomal RNA processing, Nucleic Acids Res. 31 (2003) 6148–6156.
[38] M. Holzel, M. Rohrmoser, M. Schlee, T. Grimm, T. Harasim, A. Malamoussi, A. Gruber-Eber, E. Kremmer, W. Hiddemann, G.W. Bornkamm, D. Eick, Mammalian WDR12 is a novel member of the Pes1-Bop1 complex and is required for ribosome biogenesis and cell proliferation, J. Cell Biol. 170 (2005) 367–378.
[39] S. Boudjadi, J.C. Carrier, J.F. Groulx, J.F. Beaulieu, Integrin alpha1beta1 expression is controlled by c-MYC in colorectal cancer cells, Oncogene 35 (2016) 1671–1678.
[40] R. Adam, R.J. de Haas, D.A. Wicherts, E. Vibert, C. Salloum, D. Azoulay, D. Castaing, Concomitant extrahepatic disease in patients with colorectal liver metastases: when is there a place for surgery? Ann. Surg. 253 (2011) 349–359.
[41] H. Brenner, M. Kloor, C.P. Pox, Colorectal cancer, Lancet 383 (2014) 1490–1502.
[42] S.D. Richman, M.T. Seymour, P. Chambers, F. Elliott, C.L. Daly, A.M. Meade, G. Taylor, J.H. Barrett, P. Quirke, KRAS and BRAF mutations in advanced colorectal cancer are associated with poor prognosis but do not preclude benefit from oxaliplatin or irinotecan: results from the MRC FOCUS trial, J. Clin. Oncol. 27 (2009) 5931–5937.
[43] L. Kriegl, M. Vieth, T. Kirchner, A. Menssen, Up-regulation of c-MYC and SIRT1 expression correlates with malignant transformation in the serrated route to colorectal cancer, Oncotarget 3 (2012) 1182–1193.
[44] E. Lemieux, S. Cagnol, K. Beaudry, J. Carrier, N. Rivard, Oncogenic KRAS signalling promotes the Wnt/beta-catenin pathway through LRP6 in colorectal cancer, Oncogene 34 (2015) 4914–4927.
[45] D. Lea, S. Haland, H.R. Hagland, K. Soreide, Accuracy of TNM staging in colorectal cancer: a review of current culprits, the modern role of morphology and stepping-stones for improvements in the molecular era, Scand. J. Gastroenterol. 49 (2014) 1153–1163.
[46] M.J. Duffy, Personalized treatment for patients with colorectal cancer: role of biomarkers, Biomark. Med. 9 (2015) 337–347.
[47] L. Soucek, J.R. Whitfield, N.M. Sodir, D. Masso-Valles, E. Serrano, A.N. Karnezis, L.B. Swigart, G.I. Evan, Inhibition of Myc family proteins eradicates KRas-driven lung cancer in mice, Genes Dev. 27 (2013) 504–513.
[48] P. Filippakopoulos, J. Qi, S. Picaud, Y. Shen, W.B. Smith, O. Fedorov, E.M. Morse, T. Keates, T.T. Hickman, I. Felletar, M. Philpott, S. Munro, M.R. McKeown, Y. Wang, A.L. Christie, N. West, M.J. Cameron, B. Schwartz, T.D. Heightman, N. La Thangue, C.A. French, O. Wiest, A.L. Kung, S. Knapp, J.E. Bradner, Selective inhibition of BET bromodomains, Nature 468 (2010) 1067–1073.